FRACTURE TESTS OF MULTIPLE SPECIMEN SIZES: MECHANICAL FRACTURE PARAMETERS OF C30/37 CONCRETE BY INVERSE ANALYSIS

Martin LIPOWCZAN, Martina ŠOMODÍKOVÁ, David LEHKÝ

Institute of Structural Mechanics, Faculty of Civil Engineering, Brno University of Technology,
Veveri 95, Brno 602 00, Czech Republic

lipowczan.m@fce.vutbr.cz, somodikova.m@fce.vutbr.cz, lehky.d@fce.vutbr.cz

DOI: 10.35181/tces-2021-0012

Abstract. *The paper presents a part of the research aimed at developing a comprehensive experimental–computational methodology for determining the values of mechanical fracture parameters of concrete independent of the specimen size and geometry. To this end, laboratory fracture tests in three-point bending and wedge-splitting test configurations were carried out using three different specimen sizes with two well-separated initial notch depths. The test records were used to identify selected mechanical fracture parameters using inverse analysis. Identifications were performed for individual specimens of each test configuration followed by statistical evaluation for individual sizes, notch depths, test configurations and for all specimens tested. The obtained parameters were used in the numerical simulation of the tests and the resulting load vs. displacement diagrams were compared with the experimental ones. The parameters were also analysed in terms of their dependence on the size of the initial uncracked ligament. As expected, a significant dependence of the fracture parameters was confirmed.*

Keywords

C30/37 concrete, inverse analysis, mechanical fracture parameters, size effect, three-point bending test, wedge splitting tests.

1. Introduction

Advanced reliability and durability assessment of concrete structures supported by numerical simulation requires knowledge of the corresponding mechanical and fracture parameters. These can be obtained from fracture laboratory tests of specimens in suitable configurations, either by direct evaluation of the obtained test records [1], [2], [3] or indirectly by inverse analysis [4], [5]. When obtaining the parameters, it should be taken into account that the determined values are dependent on the shape and size of the test specimen as demonstrated and analysed by several authors in the last decades, e.g. [6], [7], [8], [9], and should be viewed as contractual comparative values.

To verify the effect of specimen size and geometry on the fracture energy and other mechanical fracture parameters, a comprehensive multilevel approach for experimental–computational determination of mechanical fracture parameters of concrete is being developed. This includes testing, advanced evaluation and soft computing-based identification of specimens of multiple sizes in multiple test configurations and analyses of fracture processes using multiscale modelling approaches. In the paper, the results of the determination of mechanical fracture parameters using artificial neural network-based inverse analysis [4], [5] and records of three-point bending and wedge splitting tests using different specimen sizes and initial notch depths are presented.

2. Laboratory Tests

The extensive experimental program was carried out. It consisted of simultaneously performed three-point bending tests (3PBT) and wedge-splitting tests (WST) using three different specimen sizes in the ratio 1:3 and with two well-separated depths of notches. The shallow initial notches have a relative notch depth of $a_0/D = 0.2$, where a_0 is the notch depth and D is the overall depth of the specimen. The value for the deep notches was 0.5. Note that in the case of the smallest WST specimens, the shallow notches were omitted due to the required cut-out size for seating the jigs and wedge. Three specimens were tested for each testing case apart from the smallest WST specimens with the deep notches, in this instance 6 specimens were tested.

Nominal depths D of prismatic specimens tested in 3PBT configuration were 100, 200, and 300 mm. Lengths

of specimens were 4*D*, loading spans were 3*D*, see Fig. 1 top. Specimens for WST had the same nominal length and depth *D* equal to 100, 200, and 300 mm, see Fig. 1 bottom. All specimens for both 3PBT and WST, respectively, had the same width of 100 mm, i.e. specimen sizes differed only in two dimensions. In total, 36 specimens were tested during the main testing campaign.

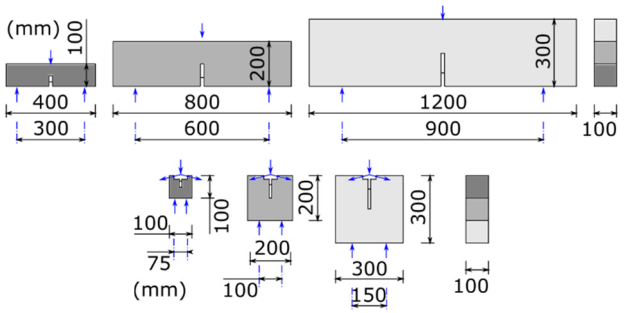

Fig. 1: Specimen of three different sizes each with shallow and deep notch tested in three-point bending (top) and wedge splitting (bottom) test configurations.

In this paper, the individual specimens are labelled with respect to the above-mentioned attributes as follows. The first letter indicates the test configuration and can be either "B" for 3PBT or "W" for WST. The number in the second position indicates the nominal depth *D* of the specimen, which is either 100, 200, or 300. The letter in the third position indicates the depth of the initial notch and can be either "S" as a shallow or "L" for a deep (large) notch.

All specimens were made of the same concrete mixture which was designed to be of C30/37 strength class which is widely used in engineering practice. The maximum aggregate grain size was 16 mm, water to cement ratio was 0.54, the cement matrix was manufactured using the CEM 42.5 R Portland cement. Specimens were stored in wet conditions with RH > 90 % for the whole time of ageing. An average bulk density of hardened concrete at 97 days was 2320 kg/m^3. The process of concrete ageing and development of its mechanical properties was analysed by performing compression tests, splitting tensile tests, and non-destructive tests based on the resonance method for the determination of dynamic modulus of elasticity. The accompanying tests were carried out at different ages of hardening.

Both 3PBT and WST specimens were tested within one week at approximately 100 days of hardening. Both tests were conducted using the stiff multi-purpose mechanical testing machine LabTest 6.250 with the load range of 0–250 kN. The loading process was governed by a constant increment of displacement of 0.02 mm/min during the entirety of testing. Examples of both test configurations are depicted in Fig. 2. WST setup was according to [10]. In the case of 3BPT, the vertical displacement was measured using the inductive sensor mounted in a special measurement frame placed on a top surface of the specimens (see Fig. 2 left). Crack mouth opening displacement (CMOD) was measured using a displacement transducer mounted between blades fixed on the bottom surface of the test specimens, close to the initial notch. In the case of WST, the CMOD was measured in the horizontal axis of the bearings using the inductive sensors mounted symmetrically to the central axis of the test specimens. The sensors were fixed in a special measuring frame placed on a top surface of the specimens (see Fig. 2 right).

Fig. 2: Test configurations of a three-point bending test (left) and wedge-splitting test (right).

Figure 3 shows examples of cracked specimens after 3PBT and WST were performed. In both configurations, the main crack progressively develops as the specimen is loaded, propagating from the top of the edge notch towards the free boundary of the specimen. Two new fractal surfaces are formed at the final failure (Fig. 4).

Fig. 3: Examples of cracked specimens tested in three-point bending (left) and wedge splitting (right) test configurations.

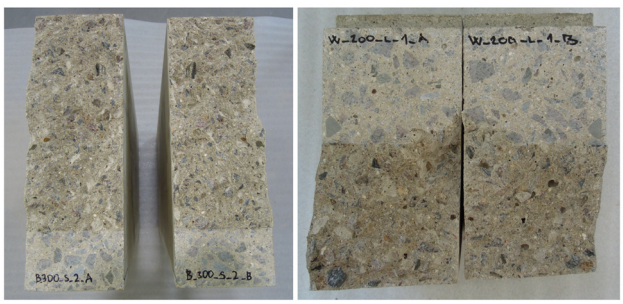

Fig. 4: Cracked surfaces after final failure of specimens tested in three-point bending (left) and wedge splitting (right) tests.

The outcome of each test is a vertical force vs. midspan deflection diagram (in the case of 3PBT) and vertical force vs. CMOD (in the case of WST). In the case of WST, it is necessary for the further determination of mechanical fracture parameters to recalculate the vertical force F_v to horizontal splitting force F_{sp} according to:

$$F_{sp} = \frac{F_v}{2\mathrm{tg}\theta}, \qquad (1)$$

where θ is the half-angle of the splitting wedge; in this case, $\theta = 30°/2 = 15°$. Figures 6 and 7 show the limits of the 95% confidence interval of the experimentally

obtained diagrams for all tested sets (dashed lines). For more details on concrete mixture, pilot tests, accompanying tests and resulting values of selected mechanical fracture parameters obtained by direct evaluation of test records see [11].

3. Parameter Identification

In tandem with the direct evaluation of the mechanical fracture parameters from the fracture test records, the results of which are presented in [11], parameter identification was carried out using an inverse analysis based on an artificial neural network. An inverse procedure developed by Novák and Lehký [4] transforms fracture test response data into the desired mechanical fracture parameters. This approach is based on matching laboratory measurements with the results gained by reproducing the same test numerically [5]. The ATENA FEM programme [12] was employed for the numerical simulation of the fracture tests. The "3D NonLinear Cementitious 2" material model was selected to govern the gradual evolution of localized damage. The tensile softening of the material is described using an exponential model according to [13]. The fracture model employs the orthotropic smeared crack formulation and the fully rotated crack model with the mesh adjusted softening modulus both in tension and compression. This model is defined on the basis of characteristic element dimensions in tension and compression to ensure the objectivity in the strain-softening regime. Further details are available in [12]. Figure 5 shows finite element meshes adopted for the smallest and the largest specimens in both test configurations. The model dimensions and the type and location of supports complies with the actual tested specimens displayed in Fig. 1. The analysis was performed under plane stress conditions.

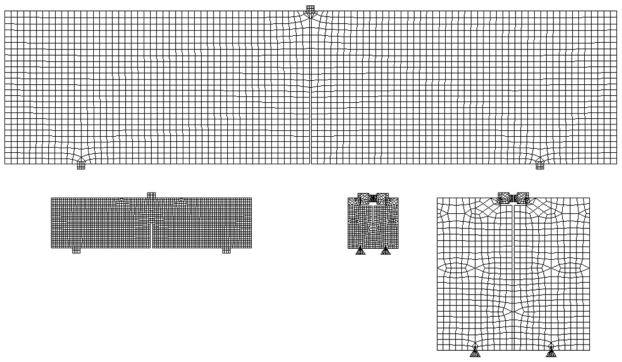

Fig. 5: Finite element models of the smallest and the largest specimens tested in three-point bending and wedge splitting tests.

The cornerstone of the inverse method is the artificial neural network (ANN), which is used as a surrogate model of an unknown inverse function between the input mechanical fracture parameters and the corresponding response parameters. Three material parameters were subject identification – modulus of elasticity E, tensile strength f_t, and fracture energy G_f. A set of numerical FEM analyses was performed with the randomly generated realizations of material parameters to provide a random response of the test specimen. The random realizations of the material parameters together with the random response parameters of the structure were used as the training set for the neural network whose parameters are optimized. With a suitably chosen stochastic model, the obtained responses well represent the range of experiments performed and contribute to good convergence in network training and subsequent identification.

Once the network was properly trained to respond to the input information (random response) with the corresponding output (material parameters), it was simulated with the experimental response as its input. The output of the simulation is the set of identified material parameters. With the obtained parameters, a validation numerical simulation was performed and compared with the experimental measurements.

4. Results

4.1. Mechanical Fracture Parameters

The mechanical fracture parameters were successively identified for all 36 specimens tested in 3PBT and WST configurations. Values of modulus of elasticity E, tensile strength f_t, and fracture energy G_f are summarized in Tabs. 1 and 2 together with the mean value (in bold) and coefficients of variation (in parentheses) for each tested set and also for all tested specimens. Note that a number in specimen name indicates its nominal depth while "L" and "S" stand for the deep, and shallow notch.

Tab.1: Identified values, mean values (in bold) and coefficients of variation (in parentheses) of modulus of elasticity, tensile strength, and fracture energy for specimens tested in the 3PBT.

Specimen	Modulus of elasticity E (GPa)		Tensile strength f_t (MPa)		Fracture energy G_f (J/m^2)	
B_100_L	28.63 29.72 28.24	**28.86** (2.7)	4.22 4.47 3.46	**4.05** (13.0)	169.22 121.82 185.33	**158.79** (20.8)
B_100_S	32.10 35.37 32.64	**33.37** (5.3)	3.62 3.75 2.58	**3.32** (19.4)	166.77 192.56 169.88	**176.41** (8.0)
B_200_L	29.00 31.35 29.94	**30.09** (3.9)	2.83 2.60 3.54	**2.99** (16.4)	187.32 214.86 235.26	**212.48** (11.3)
B_200_S	32.00 35.31 32.53	**33.28** (5.3)	2.84 2.50 2.31	**2.55** (10.5)	213.71 208.99 193.79	**205.49** (5.1)
B_300_L	35.07 36.31 34.28	**35.22** (2.9)	3.15 3.36 2.98	**3.17** (6.0)	246.81 193.90 196.58	**212.43** (14.0)
B_300_S	37.96 36.94 36.96	**37.29** (1.6)	2.57 2.20 2.41	**2.39** (7.7)	241.25 221.75 218.04	**227.01** (5.5)
B_all		**33.02** (9.5)		**3.08** (21.5)		**198.77** (15.4)

Tab.2: Identified values, mean values (in bold) and coefficients of variation (in parentheses) of modulus of elasticity, tensile strength, and fracture energy for specimens tested in the WST.

Specimen	Modulus of elasticity E (GPa)		Tensile strength f_t (MPa)		Fracture energy G_f (J/m^2)	
W_100_L	28.49 28.31 32.70 30.53 29.69 32.48	**30.37** (6.3)	2.83 3.69 3.61 3.84 3.48 3.86	**3.55** (10.7)	160.81 155.56 149.42 140.52 142.00 132.23	**146.76** (7.2)
W_200_L	23.58 25.55 21.61	**23.58** (8.4)	2.84 3.48 3.79	**3.37** (14.4)	209.05 185.38 193.13	**195.85** (6.2)
W_200_S	26.81 37.73 29.37	**31.30** (18.2)	3.02 2.32 2.91	**2.75** (13.6)	235.41 166.63 161.93	**187.99** (21.9)
W_300_L	28.70 28.59 28.43	**28.57** (0.5)	2.97 3.13 3.42	**3.17** (7.3)	199.40 219.45 201.92	**206.92** (5.3)
W_300_S	37.96 32.78 33.45	**34.73** (8.1)	2.47 2.35 2.74	**2.52** (8.0)	254.34 233.50 224.26	**237.37** (6.5)
W_all		**29.82** (14.3)		**3.15** (16.2)		**186.94** (20.0)

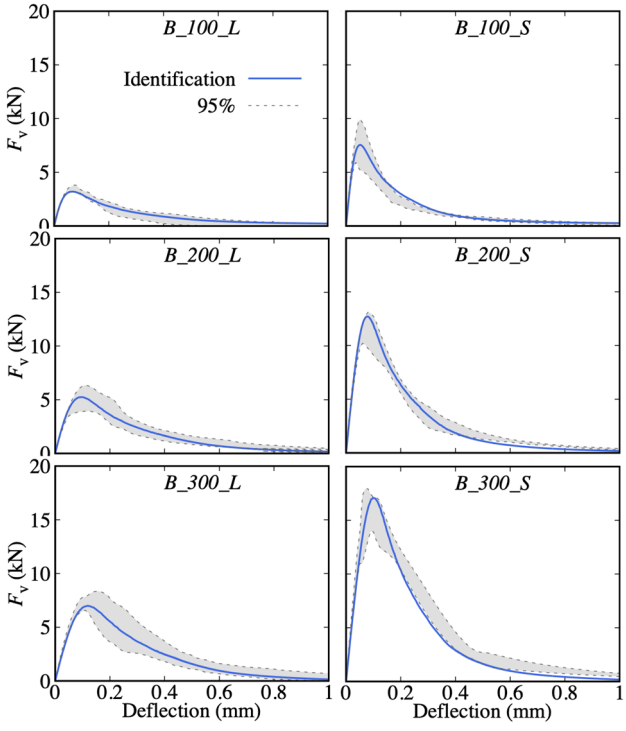

Fig. 6: Vertical force vs. deflection diagrams obtained from the numerical simulation of the 3PBT with the mean values of the identified parameters from all tested specimens and their comparison with the 95% confidence interval of the experimental values.

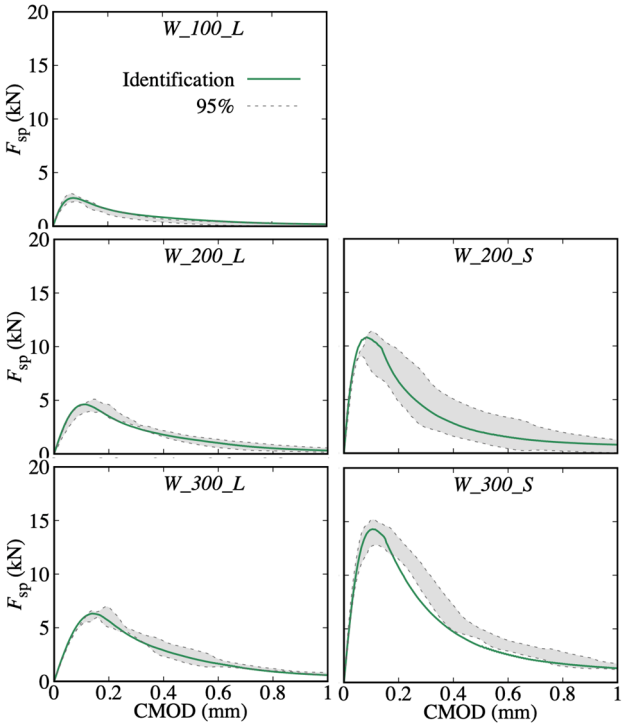

Fig. 7: Splitting force vs. crack mouth opening displacement diagrams obtained from the numerical simulation of the WST with the mean values of the identified parameters from all tested specimens and their comparison with the 95% confidence interval of the experimental values.

Resulting mean values (coefficients of variation) of C30/37 concrete, obtained from all tested 3PBT and WST specimens, are:

- E = 31.42 GPa (12.8 %)
- f_t = 3.12 MPa (18.7 %)
- G_f = 192.85 J/m^2 (17.7 %)

These values were used in the numerical simulations of all eleven test configurations (6 × 3PBT + 5 × WST) and the obtained force vs. displacement diagrams were compared with the 95% confidence interval of the values obtained from the experiments, see Figs. 6 and 7. In all cases, a very good agreement between simulated and experimental response was obtained.

4.2. Size-Dependency of Parameters

When comparing the values of the parameters in Tabs. 1 and 2 obtained for different specimen sizes, a certain degree of dependence on the size of the tested specimen, more precisely on the size of the initial uncracked ligaments, is evident. Figures 8–10 depict obtained values of modulus of elasticity, tensile strength, and fracture energy, all plotted against the depth of the initial uncracked ligament. Note that the 300_L specimens have slightly smaller ligament depth (150 mm) than the 200_S specimens (160 mm), even if the specimen itself is bigger.

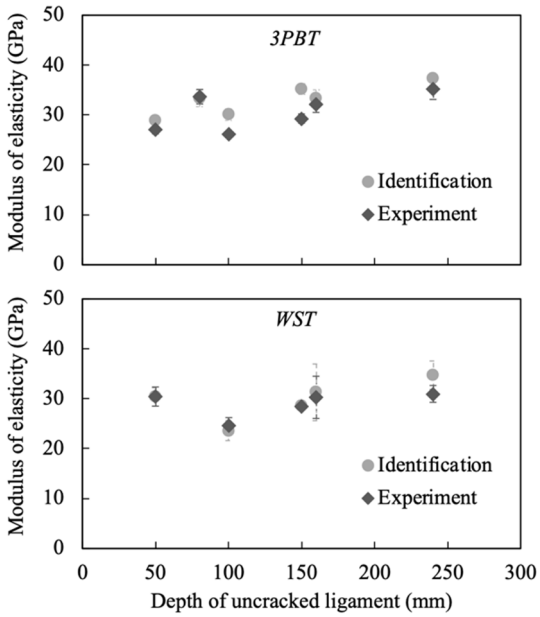

Fig. 8: Dependence of modulus of elasticity on the size of the uncracked ligament: identification vs. experiment for 3PBT (top) and WST (bottom) specimens.

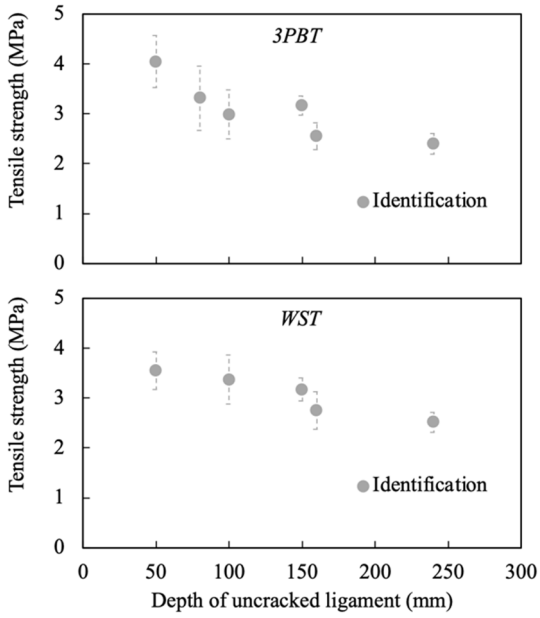

Fig. 9: Dependence of tensile strength on the size of the uncracked ligament for 3PBT (top) and WST (bottom) specimens.

Figures 8 and 10 also shows the results of the experimental evaluation of the modulus of elasticity and fracture energy obtained using the Effective crack model and the Work-of-fracture method, see [4] for details. Note that the tensile strength cannot be obtained by direct evaluation of experiments so inverse analysis is the ideal way to determine it. Reflecting the variability, the results obtained are in very good agreement with those obtained by direct evaluation of the fracture test records. This is true except for the G_f for the largest WST specimens. The analysis of their test records showed a certain degree of instability in the softening part of the loading diagram. Thus, the G_f values may be overestimated.

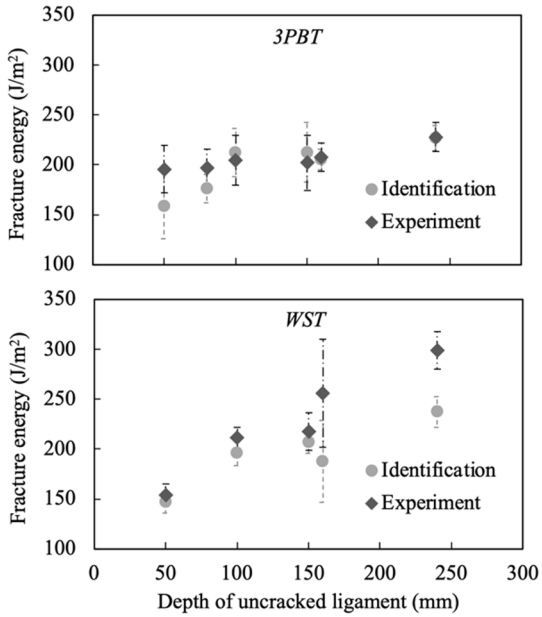

Fig. 10: Dependence of fracture energy on the size of the uncracked ligament: identification vs. experiment for 3PBT (top) and WST (bottom) specimens.

The identification results confirmed the findings from the fracture tests, which is the dependence of the fracture energy on the specimen size (see the slope of the linear regression in Fig. 10) since its value is influenced by the size of the fracture process zone, which in turn is influenced by the free boundary of the test specimen. A size dependence was also confirmed for the tensile strength. On the other hand, the results confirmed the independence of the modulus of elasticity on the size of the tested specimens.

5. Conclusion

The present contribution summarizes the identification part of the project concerned with the development of a comprehensive multilevel approach for the experimental–computational determination of the mechanical fracture parameters of concrete. Three-point bending and wedge-splitting tests were performed simultaneously using three different geometrically similar specimen sizes and two well-separated depths of initial notches. An artificial neural network method was then successfully applied to identify the basic material parameters of concrete needed in most available constitutive models. An integral part of the analysis of the results from multiple tests is to respect the natural variability of the results, as can be seen by comparing the force versus displacement diagrams with the 95% confidence interval of the experimental values. Although the specimens are all made of the same concrete, each one represents a unique realization in terms of statistics, and therefore it is not possible to match diagrams for different specimen sizes or different notch depths, but it is necessary to work with a probability distribution.

When comparing the results from the three-point

bending tests and the wedge-splitting tests, there is very good agreement in the obtained parameter values. Thus, in order to obtain size-independent fracture properties, it can be recommended, as a minimalist option, to perform fracture tests of either of these two test configurations on specimens of at least one size but with two well-separated depths of initial notches, followed by the back-calculation procedure according to Abdalla and Karihaloo. Based on the results, specimens with a nominal depth of 200 mm can be recommended. The size of their initial uncracked ligament is sufficiently large even with a deep notch and the fracture process is then not so much affected by the specimen free boundary. However, the disadvantage may be the greater power requirements of the testing machine and the greater weight of the specimen and therefore more difficult handling, especially in the case of 3PBT specimens.

Acknowledgements

The authors would like to express their thanks for the support provided from the Czech Science Foundation project MUFRAS No. 19-09491S and the specific university research project No. FAST-J-21-7552 granted by Brno University of Technology. Special thanks are addressed to Barbara Kucharczyková and Petr Daněk from Brno University of Technology for conducting the fracture tests whose results were used in the applications section of this paper.

References

[1] RILEM TC – 50 FMC. Determination of the fracture energy of mortar and concrete by means of three-point bend tests on notched beams. *Materials and Structures*. 1985, vol. 18, iss. 4, pp. 287–290.

[2] KARIHALOO, B. L. *Fracture Mechanics and Structural Concrete*. Harlow, Essex, England: Longman Scientific & Technical, 1995.

[3] ABDALLA, H. M. and B. L. KARIHALOO. Determination of size-independent specific fracture energy of concrete from three-point bend and wedge splitting tests. *Magazine of Concrete Research*. 2003, vol. 55, pp. 133–141.

[4] NOVÁK, D. and D. LEHKÝ. ANN Inverse Analysis Based on Stochastic Small-Sample Training Set Simulation. *Engineering Application of Artificial Intelligence*. 2006, vol. 19, pp. 731–740. DOI: 10.1016/j.engappai.2006.05.003.

[5] LEHKÝ, D., Z. KERŠNER and D. NOVÁK. FraMePID-3PB Software for Material Parameters Identification Using Fracture Test and Inverse Analysis. *Advances in Engineering Software*. 2014, vol. 72, pp. 147–154. ISSN 0965-9978, DOI: 10.1016/j.advengsoft.2013.10.001.

[6] NALLATHAMBI, P., B. L. KARIHALOO and B. S. HEATON. Various size effect in fracture of concrete. *Cement and Concrete Composites*. 1985, vol. 15, pp. 117–126.

[7] BAŽANT, Z. P. and M. T. KAZEMI. Size dependence of concrete fracture energy determined by RILEM work-of- fracture method. *International Journal of Fracture*. 1991, vol. 51, pp. 121–138.

[8] HU, X. Z. and F. H. WITTMANN. Fracture energy and fracture process zone. *Materials and Structures*. 1992, vol. 25, pp. 319–326.

[9] CARPINTERI, A. and B. CHIAIA. Size effects on concrete fracture energy: dimensional transition from order to disorder. *Material and Structures*. 1996, vol. 29, pp. 259–266.

[10] TSCHEGG, E. K. New equipment for fracture tests on concrete. *Materialprüfung/Materials Testing.* 1991, vol. 33, pp. 338–343.

[11] LEHKÝ, D., B. KUCHARCZYKOVÁ, H. ŠIMONOVÁ and P. DANĚK. Comprehensive fracture tests of concrete for the determination of mechanical fracture parameters. *Structural Concrete*. 2020. DOI: 10.1002/suco.202000496.

[12] ČERVENKA, V., L. JENDELE and J. ČERVENKA. *ATENA program documentation Part 1: theory*. Prague: Červenka Consulting Ltd., 2016.

[13] HORDIJK, D. A. *Local approach to fatigue of concrete*. Delft, 1991. Ph.D. thesis. Technische Universiteit Delft. Supervisor: H. W. Reinhardt.

About Authors

Martin LIPOWCZAN was born in Frýdek-Místek, Czech Republic. He received his M.Sc. degree in Civil Engineering in 2018. His research interests include identification of mechanical fracture parameters, fracture mechanics and utilization of soft computing methods in structural engineering.

Martina ŠOMODÍKOVÁ was born in Prostějov, Czech Republic. She received her doctoral degree (Ph.D.) from Constructions and Traffic Structures in 2016. Her research interests include approximation methods for determining the reliability of structures, modelling of degradation processes in concrete and stochastic computational mechanics.

David LEHKÝ was born in Moravský Krumlov, Czech Republic. He received his Associate Professor degree in Structures and Infrastructure Engineering in 2017. He conducts research in structural safety and reliability quantification, nonlinear fracture mechanics modelling and utilization of soft computing methods for solving inverse problems in materials and structural engineering.